

Delayed cutaneous wound closure in HO-2 deficient mice despite normal HO-1 expression

Ditte M. S. Lundvig ^{a, #}, Alwin Scharstuhl ^{b, #}, Niels A. J. Cremers ^a, Sebastiaan W. C. Pennings ^a, Jeroen te Paske ^b, René van Rheden ^a, Coby van Run-van Breda ^a, Raymond F. Regan ^c, Frans G. M. Russel ^b, Carine E. Carels ^a, Jaap C. Maltha ^a, Frank A. D. T. G. Wagener ^{a, *}

^a Department of Orthodontics and Craniofacial Biology, Radboud Institute for Molecular Life Sciences, Radboud University Medical Center, Nijmegen, The Netherlands

^b Department of Pharmacology and Toxicology, Radboud Institute for Molecular Life Sciences, Radboud University Medical Center, Nijmegen, The Netherlands

^c Department of Emergency Medicine, Thomas Jefferson University, Philadelphia, PA, USA

Received: March 3, 2014; Accepted: June 30, 2014

Abstract

Impaired wound healing can lead to scarring, and aesthetical and functional problems. The cytoprotective haem oxygenase (HO) enzymes degrade haem into iron, biliverdin and carbon monoxide. HO-1 deficient mice suffer from chronic inflammatory stress and delayed cutaneous wound healing, while corneal wound healing in HO-2 deficient mice is impaired with exorbitant inflammation and absence of HO-1 expression. This study addresses the role of HO-2 in cutaneous excisional wound healing using HO-2 knockout (KO) mice. Here, we show that HO-2 deficiency also delays cutaneous wound closure compared to WT controls. In addition, we detected reduced collagen deposition and vessel density in the wounds of HO-2 KO mice compared to WT controls. Surprisingly, wound closure in HO-2 KO mice was accompanied by an inflammatory response comparable to WT mice. HO-1 induction in HO-2 deficient skin was also similar to WT controls and may explain this protection against exaggerated cutaneous inflammation but not the delayed wound closure. Proliferation and myofibroblast differentiation were similar in both two genotypes. Next, we screened for candidate genes to explain the observed delayed wound closure, and detected delayed gene and protein expression profiles of the chemokine (C-X-C) ligand-11 (CXCL-11) in wounds of HO-2 KO mice. Abnormal regulation of CXCL-11 has been linked to delayed wound healing and disturbed angiogenesis. However, whether aberrant CXCL-11 expression in HO-2 KO mice is caused by or is causing delayed wound healing needs to be further investigated.

Keywords: haem oxygenase • wound healing • skin

Introduction

Cutaneous wound repair occurs in temporally coordinated and overlapping phases: inflammation, granulation tissue formation and remodelling [1]. The timely progression of the different phases is coordinated by cytokines and growth factors, and each phase is

characterized by the presence of specific cell types [2]. Both clinical and experimental studies have confirmed the importance for a well-regulated inflammatory resolution for proper wound healing, since prolonged inflammatory and oxidative stress may cause non-healing, chronic wounds or excessive scarring [3, 4].

Haem oxygenases (HO) are enzymes that degrade haem into biliverdin, carbon monoxide and iron. Biliverdin is then converted into the antioxidant bilirubin by biliverdin reductase. HO-1 is highly inducible by a wide range of stresses, including inflammatory and oxidative stress, whereas HO-2 is mainly constitutively expressed [5, 6]. The HO system is important in the resolution of inflammation [7, 8]. The cytoprotective effects of the stress-induced HO-1 are evident in various pathological models and settings, whereas the constitutive

#Contributed equally.

*Correspondence to: Frank A. D. T. G. WAGENER, Department of Orthodontics and Craniofacial Biology, Radboud university medical center, PO Box 9101, Nijmegen 6500 HB, The Netherlands.

Tel.: +31-243614082

Fax: +31-243540631

E-mail: frank.wagener@radboudumc.nl

doi: 10.1111/jcmm.12389

© 2014 The Authors.

Journal of Cellular and Molecular Medicine published by John Wiley & Sons Ltd and Foundation for Cellular and Molecular Medicine.

This is an open access article under the terms of the Creative Commons Attribution License, which permits use, distribution and reproduction in any medium, provided the original work is properly cited.

HO-2 is important for physiological maintenance of the haem pool [9].

HO-1 deficient humans and mice demonstrate chronic inflammatory stress accompanied by increased leucocyte recruitment [10, 11]. Moreover, genetic or pharmacologic ablation of HO-1 expression and activity in mice results in slower cutaneous wound closure [12]. Also, HO-2 deficient mice show delayed wound healing and an exaggerated inflammatory response after corneal epithelial wounding [13, 14] which was associated with impaired HO-1 induction and function [13]. Notably, HO-2 levels have been suggested to regulate HO-1 expression and function in a cell and tissue-specific manner [15], and compensatory HO-1 expression in HO-2 deficient tissue has been reported [16, 17]. Moreover, genetic or pharmacological HO-1 induction as well as administration of HO effector molecules biliverdin/bilirubin down-regulate the inflammatory response and restore wound healing in HO-1 deficient skin [12, 18] and HO-2 deficient cornea [14, 19]. On the other hand, HO-1 has pro-angiogenic effects *via* regulating VEGF synthesis [20, 21]. Wound healing in HO-1 KO mice occurs with reduced neovascularization in the skin [12] whereas exaggerated angiogenesis was found in HO-2 deficient corneas [19]. Application of biliverdin ameliorated this pathologic angiogenesis occurring after corneal wounding in HO-2 KO mice [19].

Because of the described intricate involvement of both HO-1 and HO-2 in wound healing and regulation of inflammatory responses, this study focused on exploring the possible role of HO-2 in cutaneous wound healing using a full-thickness excisional wound model and HO-2 KO mice.

Methods and materials

Animals

Homozygote HO-2 KO mice generated by targeted disruption of the HO-2 gene [22] and WT mice were bred in-house on a mixed 129Sv x C57BL/6 background. Mice were provided with food and water *ad libitum* and maintained on a 12-hr light/dark cycle and specific

pathogen-free conditions. All experiments and protocols were approved by the institutional Radboud University Nijmegen animal experimentation committee.

Excisional wound model

Prior to wounding 6–12 weeks old female mice were shaved using an electrical clipper. The following day four full-thickness wounds were made on the back including the *panniculus carnosus* using a sterile disposable 4-mm biopsy punch (Kai Medical, Seki City, Japan) and the mice were left uncovered to heal ($n = 18/\text{genotype}$). At day 2 after wounding mice were killed, and the remaining mice ($n = 9/\text{genotype}$) were followed until day 7 ($n = 9/\text{genotype}$). For gene transcript analysis mice were wounded ($n = 12/\text{genotype}$) and killed at day 2 ($n = 6/\text{genotype}$) and day 5 ($n = 6/\text{genotype}$) after wounding. Punched out tissue at day 0 was collected as control. Wounds were collected using a disposable 6-mm biopsy punch (Kai Medical) allowing collection of the complete wound together with the surrounding normal tissue.

Wound size analysis

Wounds were digitally documented on different days with a ruler placed next to the wounds for size normalization. Wound area was measured at least twice by a blinded investigator using ImageJ (NIH) v1.44p software.

Immunohistochemistry

Tissue samples were fixed for 24 hrs in 4% paraformaldehyde and further processed for routine paraffin embedding. Sections were deparaffinized using Histosafe and rehydrated using an alcohol range. Endogenous peroxidase activity was quenched with 3% H_2O_2 in methanol for 20 min., and immunohistochemical stainings were performed and photographed as previously described [23]. Photographs were taken on a Carl Zeiss Imager Z.1 system (Carl Zeiss Microimaging GmbH, Jena, Germany). For antibodies and antigen retrievals used, see Table 1.

Table 1 Antibodies used for immunohistochemistry

Antibody	Specificity	Dilution	Antigen retrieval	Source
SPA-895	HO-1	1:800	A	Stressgen
OSA-200	HO-2	1:800	A	Stressgen
MCA497R	F4/80	1:200	A	AbD Serotec, Kidlington, UK
2233PC0	Collagen IV	1:200	A	Euro-Diagnostica, Malmo, Sweden
Sc-34785	CXCL-11	1:100	B	Santa Cruz Biotechnology, Santa Cruz, CA, USA
A2547	α SMA	1:600	A	Sigma-Aldrich, St. Louis, MO, USA

A: 10 mM citrate buffer 70°C for 10 min, followed by trypsin digestion for 7 min.

B: 10 mM citrate buffer RT, 120 min.

Semi-quantitative scoring of immunohistochemical sections

HO-1 and F4/80 immunoreactivity were evaluated as the number of positive cells (based on the percentage of positive staining) and staining intensity of four sections per animal. Extent was scored as: 0, $\leq 5\%$; 1, 6–25%; 2, 26–50%; 3, $> 50\%$. Intensity was scored as: 0, weak; 1, moderate; 2, strong. Intensity was designated as weak when only barely detectable. To correlate extent and intensity on the staining, a composite score was calculated by multiplying the individual scores of extent by intensity. Scoring was done three times by a blinded investigator. CXCL-11 immunoreactivity was evaluated by scoring a single section per animal by two independent investigators as previously described [24]. To assess α SMA immunoreactivity four sections per animal were scored twice as earlier described [25]. Vascularization was assessed twice on five high-power fields (HPF; 400 \times magnification) on four sections per animal as previously described [26]. A mean score per animal was used for further analysis.

Collagen deposition

Collagen deposition in AZAN stained wound sections (1–4 sections/mouse) was determined by image analysis using a macro built in Image J [27]. The wound area was manually defined before running the macro using the edges of the *panniculus carnosus* and epithelium as boundaries. Measurements were performed twice, and mean intensity/mm² per mouse was used for further analysis.

Assessment of mRNA expression by quantitative real-time PCR

Total RNA was extracted from skin and wound samples by using Trizol (Invitrogen, Carlsbad, CA, USA) and a RNeasy Mini kit (Qiagen, Hilden, Germany), and cDNA was produced using the iScript cDNA synthesis kit (Bio-Rad, Hercules, CA, USA). To screen for differences in gene expression profiles of wound associated genes in HO-2 KO and WT mice, pooled cDNAs synthesized from individual wounds of HO-2 KO and WT mice isolated at day 5 were tested on a Mouse Wound Healing RT² ProfilerTM PCR Array according to the manufacturer's instructions (SABiosciences,

Frederick, MD, USA). Individual cDNAs from all time-points were subsequently analysed for genes up- or down-regulated more than twofold using custom-designed primers (Table 2) and iQ SYBR Green Supermix (Invitrogen) in a CFX96 Real-Time PCR system (Bio-Rad). Relative gene expression values were evaluated using the $2^{-\Delta\Delta Ct}$ method using GAPDH as housekeeping gene [28]. Fold changes were normalized to WT mean day 0.

Western blotting

Protein was extracted from homogenized 4-mm skin biopsies in 100 μ l lysis buffer [1 mM EDTA, 0.5% Triton X-100, Complete protease inhibitor cocktail (Roche, Penzberg, Germany), 100 μ M PMSF], and Western blotting using primary antibodies against HO-1 and HO-2 (SPA-895 and OSA-200, 1:5000; Stressgen, Victoria, BC, USA) was performed as previously described [29].

Statistical analysis

Statistical analysis was performed with GraphPad Prism 4.03 software. Normal data distribution were assessed using the Kolmogorov–Smirnov test. In case of non-normality, data were transformed. Statistical differences in qPCR data, wound closure and collagen deposition were determined using Student's *t*-test with Bonferroni-correction in case of multiple testing. Semi-quantitative scores were analysed with non-parametric Mann–Whitney test or Kruskal–Wallis test with Dunn's *post hoc* test. Collagen deposition, wound closure and qPCR data are presented as mean \pm SD. Semi-quantitative scores are presented as box-and-whisker plots of median with 10–90 percentiles. $P < 0.05$ was considered statistically significant.

Results

Delayed cutaneous wound closure in HO-2 deficient mice

Prior to experimental start, we verified that HO-2 KO mice indeed were devoid of HO-2 mRNA and protein expression (Fig. S1). To

Table 2 Murine primers used for qPCR

Gene	Forward primer (5'→3')	Reverse primer (5'→3')	Reference
HO-1	CAACATTGAGCTGTTTGAGG	TGGTCTTTGTGTTCTCTGTG	—
HO-2	AAGGAAGGGACCAAGGAAG	AGTGGTGGCCAGCTTAATAG	—
TNF	CTCTTCTCATTCTGCTGTG	GAATTGTCCATCTGGCATAAC	—
CXCL-11	CACGCTGCTCAAGGCTTCCTTATG	TGTCGCAGCCGTTACTCGGGT	—
Gr-1	TGGACTCTCAGAAAGCAAAG	GCAGAGGTCTTCTTCCAACA	—
F4/80	AATCCTGTGAAGATGTGG	GAGTGTGATGCAAATGAAG	—
ACTA2	CAGGCATGGATGGCATCAATCAC	ACTCTAGCTGTGAAGTCAGTGTCG	[51]
GAPDH	GGCAAATCAACGGCACA	GTTAGTGGGGTCTCGCTCCTG	—

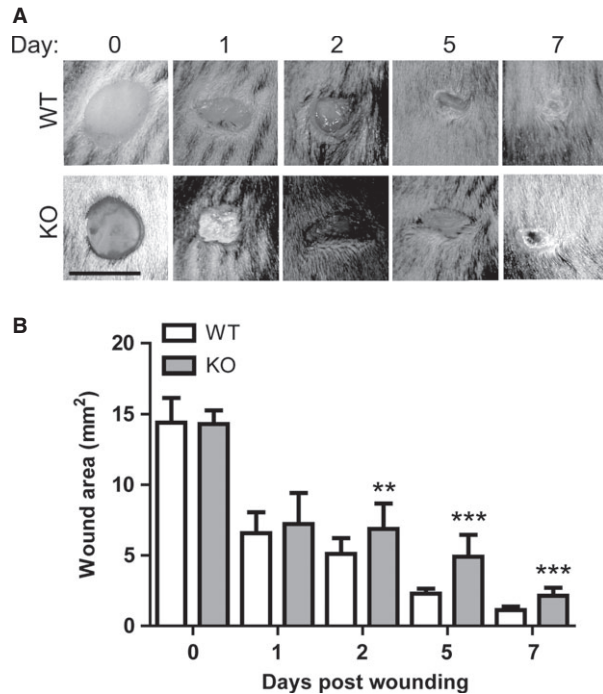


Fig. 1 Slower cutaneous wound closure in HO-2 KO after excisional wounding. **(A)** Wound closure in WT (upper panel) and HO-2 KO (lower panel) mice in time; bar, 5 mm. **(B)** Wound area (mm²) reduction in WT (white bars) and HO-2 KO (grey bars) mice in time presented as mean \pm SD. ** $P < 0.01$, *** $P < 0.001$.

investigate the role of HO-2 in cutaneous wound closure, full-thickness wounds were made on the backs of HO-2 KO and WT mice and monitored in time (Fig. 1). Wound area assessment demonstrated significantly larger wounds in HO-2 KO mice compared to WT controls at day 2 [6.9 ± 1.8 mm² versus 5.1 ± 1.1 mm² ($n = 18$ /genotype); $P < 0.01$], day 5 [4.9 ± 1.6 mm² versus 2.3 ± 0.4 mm² ($n = 9$ /genotype); $P < 0.001$] and day 7 [2.1 ± 0.6 mm² versus 1.1 ± 0.3 mm² ($n = 9$ /genotype); $P < 0.001$] after wounding.

Normal inflammatory response in HO-2 KO mice after cutaneous wounding

To determine whether delayed cutaneous wound healing in HO-2 KO mice is because of an exaggerated inflammatory response as observed after corneal injury, we compared gene expression profiles of different inflammatory factors and cell markers in skin of HO-2 KO and WT mice at day 2 and 5 (Fig. 2). The pro-inflammatory cytokine TNF and the stress-induced enzyme COX-2 demonstrated an injury-induced increase in transcript levels compared to unwounded skin in both WT and HO-2 KO mice, however, we did not detect any differences between the two genotypes at any of the investigated time-points (Fig. 2A and B). Furthermore, granulocyte marker receptor antigen-1, Gr-1 and macrophage marker F4/80 both demonstrated an

injury-induced increase in transcript levels compared to unwounded skin, however, no differences between HO-2 KO and WT mice were evident (Fig. 2C and D). This was also reflected at the protein level, as semi-quantitative assessment of F4/80 immunoreactivity in wound sections demonstrated no significant differences between HO-2 KO and WT mice at day 2 and day 7 after wounding (Fig. 2E and F).

Injury-induced HO-1 expression in both HO-2 KO and WT mice

In contrast to HO-2 deficient cornea [13] we detected both HO-1 mRNA transcript and protein in the skin of HO-2 KO mice (Fig. 3). Similar levels of HO-1 protein were detected in unwounded skin of HO-2 KO and WT mice (6.9 ± 3.2 and 9.3 ± 6.7 , respectively; Fig. 3A). Also, a comparable injury-induced increase in HO-1 transcript levels was evident in both HO-2 KO and WT mice (Fig. 3B). Furthermore, injury-induced HO-1 protein expression was detected in both WT and HO-2 KO skin (Fig. 3C). HO-1 positive cells were present at high numbers both in the wound area and in the surrounding tissue at day 2, while at day 7 HO-1 positive cells were predominantly found in the wound area (Fig. 3C). Semi-quantitative assessment of HO-1 immunoreactivity demonstrated a significant reduction in HO-1 expression at day 7 compared to day 2 in both WT and HO-2 KO wounds ($P < 0.05$ for both genotypes), however, no significant differences between the genotypes were detected (Fig. 3D).

Reduced collagen deposition and lower vessel density in HO-2 KO wounds

HO-2 KO mice demonstrated no abnormalities compared to WT mice with respect to the inflammatory phase. We therefore questioned whether the delayed wound healing was a result of a dysregulated granulation phase. Assessment of collagen deposition in wound sections of HO-2 KO and WT mice using an Image J macro demonstrated a significant lower percentage collagen deposition per area in HO-2 KO wounds compared to WT controls at day 7 after wounding ($8.8 \pm 4.2\%/mm^2$ versus $29.8 \pm 10.8\%/mm^2$, $P < 0.001$; Fig. 4A and B).

Also, we investigated the degree of vascularization in the wound areas of HO-2 KO and WT mice by semi-quantitative scoring of wound sections stained for collagen IV, a basement membrane protein found in the walls of blood vessels [30]. We detected a significant lower density of vessels per HPF in wound sections of HO-2 KO mice compared to WT mice at day 7 after wounding ($P < 0.05$; Fig. 4C and D).

We wondered if the delayed wound healing could be related to a lower cell proliferation capacity in HO-2 deficient cells, and we therefore assessed the mRNA levels of Ki67, a marker of actively cycling cells [31]. We detected a time-dependent increase in Ki67 mRNA levels consistent with an increased influx and proliferation of wound repair associated cells; however, no differences between HO-2 KO and WT mice were evident at any of the investigated time-points (Fig. 5A).

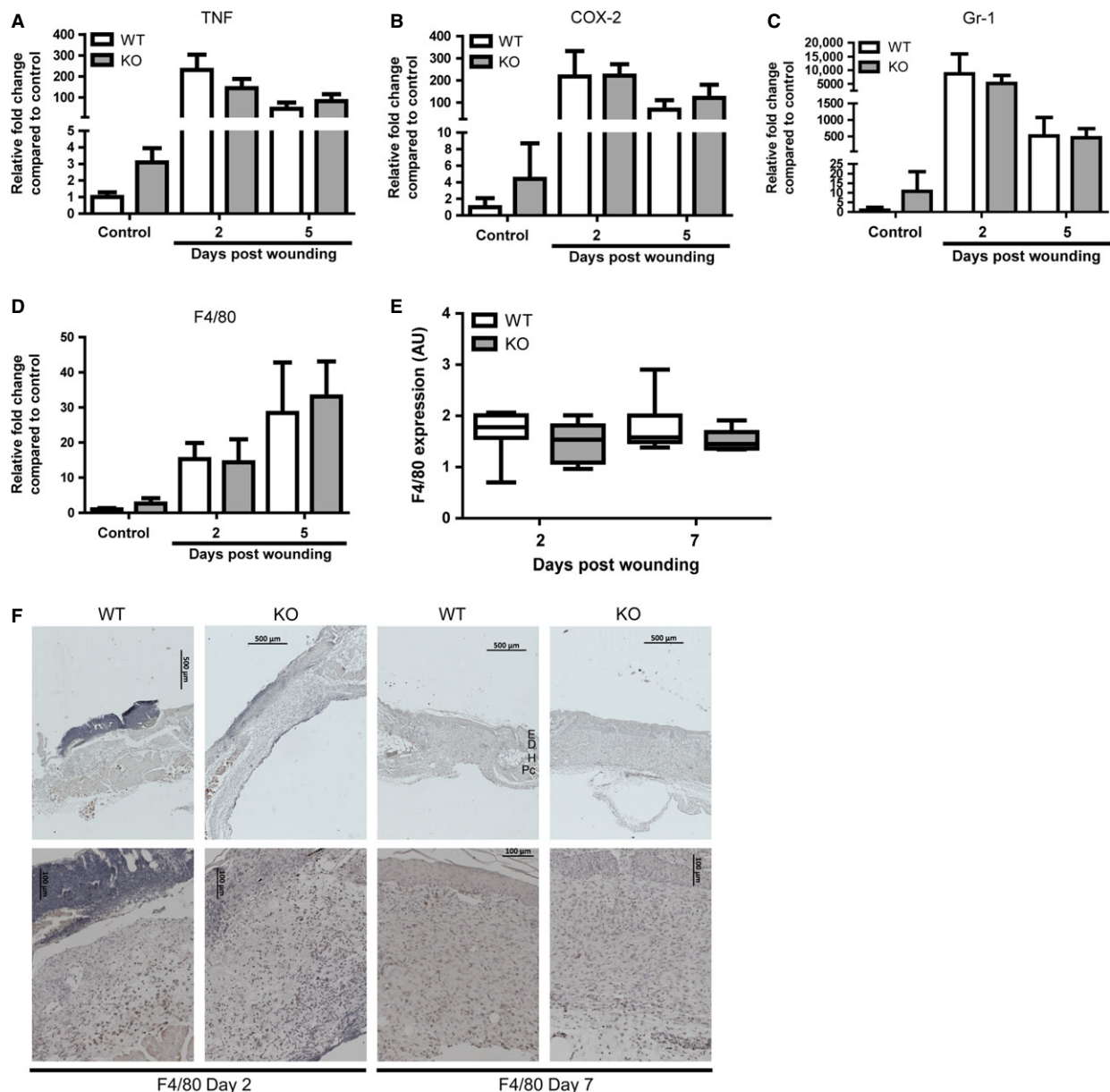
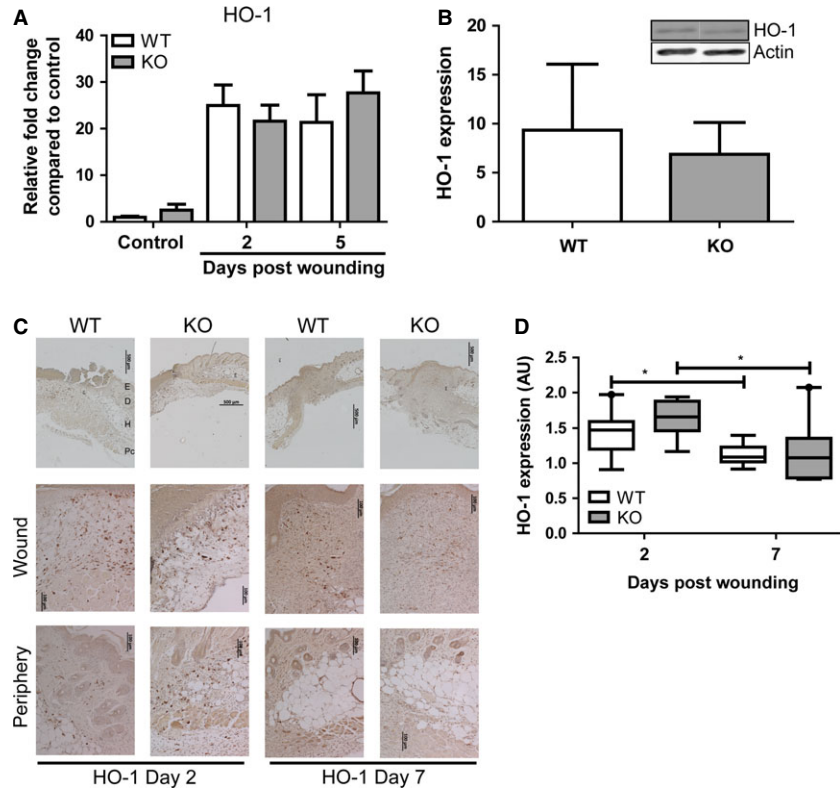


Fig. 2 HO-2 KO mice demonstrate a normal inflammatory response after wounding. Gene transcript levels of pro-inflammatory proteins (A) TNF and (B) COX-2 and inflammatory cell markers (C) Gr-1, and (D) F4/80 in WT (white bars) and HO-2 KO (grey bars) mice in time presented as mean \pm SD. Controls are tissue biopsies collected at day 0, and data were normalized to WT mean day 0. (E) Box-and-whisker plot with 10–90 percentiles of semi-quantitative assessment of F4/80 immunoreactivity in (F). (F) F4/80 immunoreactivity in representative wound sections of WT and HO-2 KO mice at day 2 and 7 after wounding. Anatomical indications by E, epidermis; D, dermis; H, hypodermis; Pc, panniculus carnosus; bars, 500 μ m (upper panel), 100 μ m (lower panel).

During the granulation phase keratinocytes dominate epithelization and (myo)fibroblasts produce ECM such as collagen and close the wound [32]. We therefore investigated whether the presence of less (myo)fibroblasts could be an explanation for the reduced collagen deposition. We detected similar mRNA levels of

ACTA2, the murine counterpart of myofibroblast marker α SMA, at all examined time-points (Fig. 5B). Moreover, we did not detect any difference in α SMA protein immunoreactivity level at day 7 after wounding as evaluated by semi-quantitative scoring (Fig. 5C and D).

Fig. 3 HO-2 KO mice induce cutaneous HO-1 expression after wounding. **(A)** HO-1 gene transcript levels in WT (white bars) and HO-2 KO (grey bars) mice in time as represented as mean \pm SD. Controls represent biopsies collected at day 0, and data were normalized to WT mean day 0. **(B)** Western blot (insert) of cutaneous HO-1 expression in unwounded skin in WT (white bar) and HO-2 KO (grey bar) mice. Band intensity was normalized to housekeeping protein β -actin. Data are presented as mean \pm SD. **(C)** HO-1 immunoreactivity in representative wound sections of WT and HO-2 KO mice at day 2 and day 7 after wounding. Anatomical indications by E, epidermis; D, dermis; H, hypodermis; Pc, panniculus carnosus; bars, 500 μ m (upper panel), 100 μ m (wound, periphery). **(D)** Semi-quantitative scores of HO-1 immunoreactivity in **(C)** presented as box-and-whisker plot with 10–90 percentiles. * $P < 0.05$.



Different expression levels of CXCL-11 in WT and HO-2 KO mice after wounding

HO-1 deficiency is linked to delayed wound healing and impaired angiogenesis after injury. However, HO-2 deficient skin demonstrates injury-induced HO-1 expression, and we therefore wondered which genes could be explanatory for the reduced collagen deposition and lower vessel density observed in HO-2 KO mice. First we compared gene expression profiles of pooled cDNAs isolated from day 5 wound tissue of HO-2 KO and WT mice using a PCR wound healing array, followed by validation by custom-designed primers and individual cDNAs. Unexpectedly, after individual validation we only detected significant differences between HO-2 KO and WT mice in the expression profile of a single gene out of 84 screened genes, namely CXCL-11 (Fig. 6A, data not shown). Injury-induced CXCL-11 gene transcription observed in WT mice was absent in HO-2 KO mice at day 2 (49.4 ± 25.3 versus 11.5 ± 5.1 ; $P < 0.05$). However, at day 5 after wounding we detected similar CXCL-11 gene transcription levels in WT and HO-2 KO mice, which was mainly because of a down-regulation of gene transcription in WT mice (Fig. 6A). In contrast, immunohistochemical staining and semi-quantitative scoring of wound tissue isolated from HO-2 KO and WT mice 7 days after wounding showed a markedly higher level of CXCL-11 positive cells in the wounds of HO-2 KO mice compared to WT controls ($P = 0.0503$; Fig. 6B and C).

Discussion

In this study, we investigated the role of HO-2 in cutaneous wound closure using HO-2 KO mice and a full-thickness excisional wound model. High levels of HO-2 in the skin have been suggested to be a first line of defense against acute injury [33]. Following excisional wounding we observed significantly slower cutaneous wound closure accompanied by reduced collagen deposition and lower vessel density in HO-2 KO mice compared to WT controls at day 7. The most pronounced difference in wound healing rates between HO-2 KO and WT seems to be during the first days of wound healing.

Cutaneous wounding is followed by haemolysis and free haem release leading to local oxidative stress and inflammation. HO-1 is rapidly induced after wounding [34, 35] and promotes inflammatory resolution by down-regulating inflammatory mediators and attenuating infiltration of inflammatory cells [36, 37]. Moreover, pharmacologic induction or overexpression of HO-1 accelerates both corneal and cutaneous wound healing [12, 38]. On the contrary, HO-1 deficiency in man and mice leads to a chronic inflammatory state [10, 11]. Also, pharmacologic or genetic inhibition of HO-1 slows down cutaneous wound closure *via* suppressed re-epithelization and neovascularization in murine models [12]. In HO-2 KO mice impaired corneal wound healing is associated with exaggerated inflammation [13, 39]. We therefore have been suggested that also the delayed

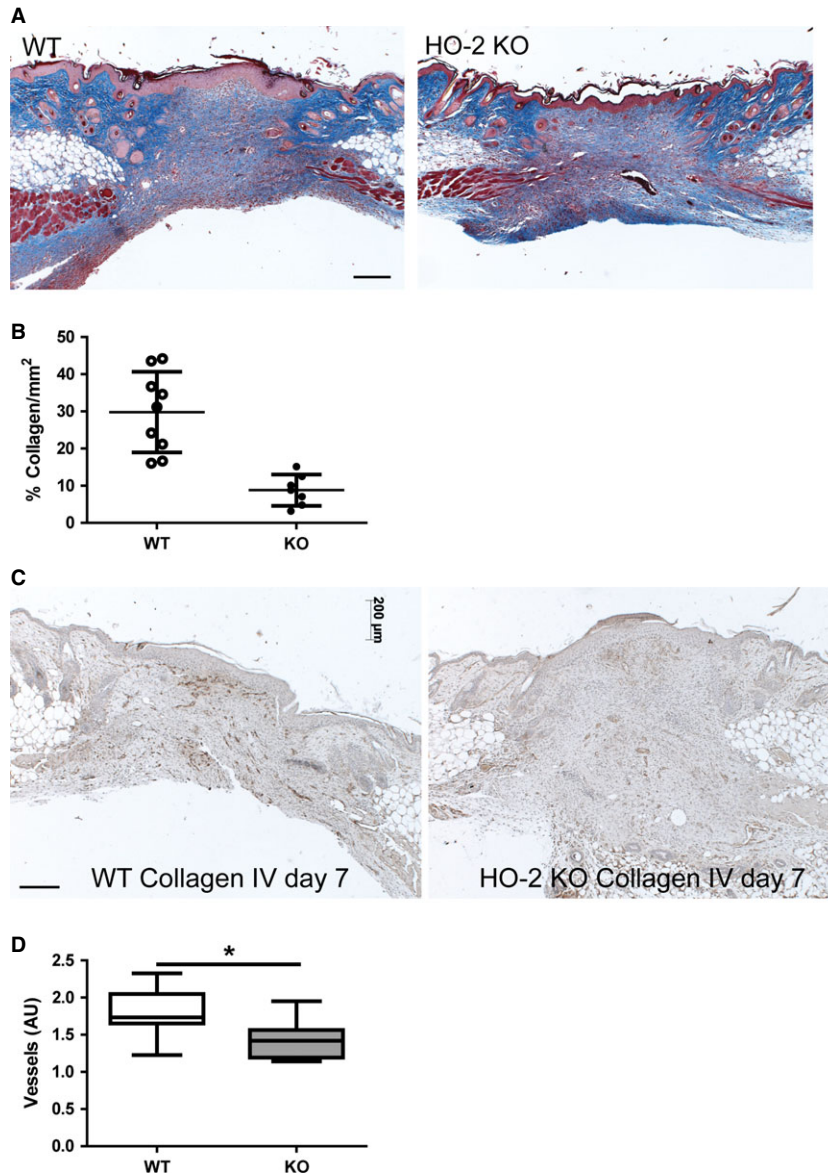


Fig. 4 Reduced collagen deposition and vessel density in HO-2 KO mice. **(A)** Representative images of AZAN stained wound sections of WT and HO-2 KO mice at day 7 after wounding; bar, 200 μ m. **(B)** Collagen deposition in WT (open circles) and HO-2 KO (closed circles) mice at day 7 after wounding. **(C)** Representative images of collagen IV immunoreactivity, a common blood vessel marker, in WT and HO-2 KO mice at day 7 after wounding; bar, 200 μ m. **(D)** Semi-quantitative scoring of high-power fields of **(C)**. Data are represented as box-and-whisker plot with 10–90 percentiles. * $P < 0.05$, *** $P < 0.001$.

cutaneous wound closure observed in HO-2 KO mice results from an exaggerated inflammatory response.

Unexpectedly, we did not detect significant differences in the mRNA or protein expression level of the pro-inflammatory proteins, such as TNF and COX-2 and markers for granulocytes and macrophages. This rules out that exaggerated inflammation is the underlying cause of delayed cutaneous wound closure in HO-2 KO mice. The exaggerated corneal inflammatory response was associated with impaired HO-1 induction and function [13]. The importance of HO-activity was further supported by amelioration of corneal inflammatory resolution after application of biliverdin in HO-2 KO mice [14, 19].

HO-2 can regulate HO-1 induction and function in a tissue and cell specific manner [15, 17]. Increased HO-1 expression has been suggested to be a compensatory mechanism in HO-2 deficient lung

and myocardium [16, 40]. We detected similar levels of both HO-1 mRNA and protein expression in unwounded skin and injury-induced HO-1 up-regulation after wounding of HO-2 KO and WT mice, explaining the normal inflammatory resolution in both genotypes. Cell-type specific compensatory HO-1 expression likely dampens the inflammatory response after cutaneous wounding, as we observed a normal inflammatory phenotype in HO-1 expressing skin compared to the exaggerated inflammatory response in HO-1 deficient corneal tissue in HO-2 KO mice [13, 39, 41]. Notably, delayed cutaneous wound closure in HO-1 KO mice is also not accompanied by an uncontrolled inflammatory response following excisional wounding [12].

We next turned our focus to the granulation phase of cutaneous wound healing that is dominated by migration, proliferation and differentiation of fibroblasts, keratinocytes and endothelial cells in the

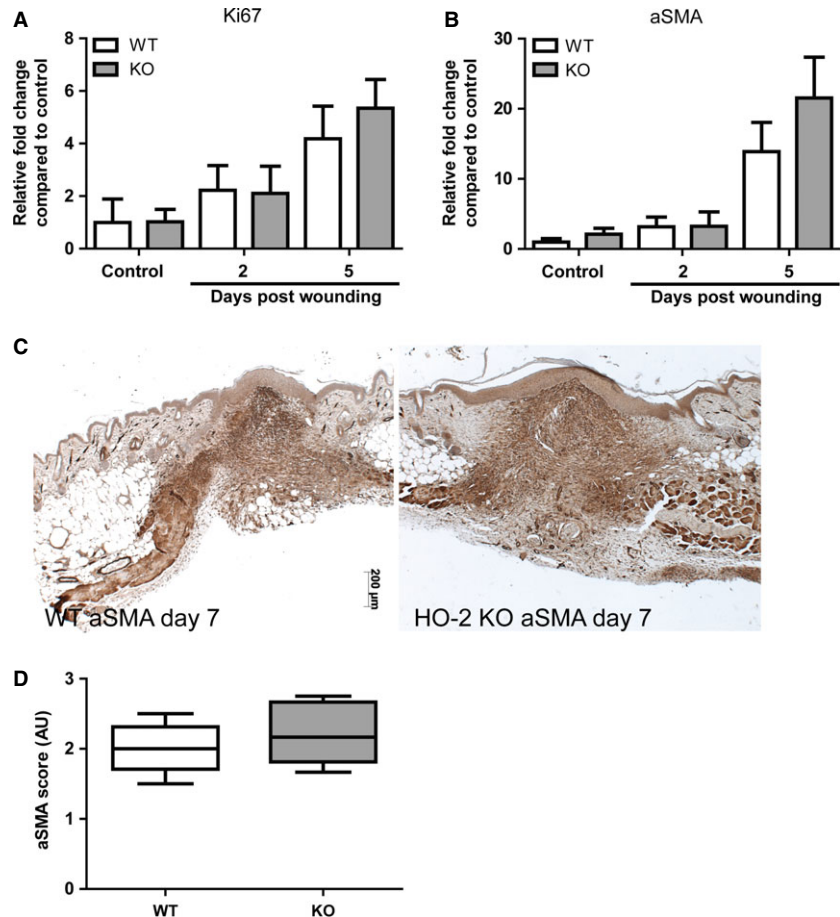


Fig. 5 Myofibroblast differentiation occurs in HO-2 KO mice. Ki67 (**A**) and ACTA2 (**B**) gene transcript levels in WT (white bars) and HO-2 KO (grey bars) mice in time as represented as mean \pm SD. Controls represent biopsies collected at day 0, and data were normalized to WT mean day 0. (**C**) Representative images of α SMA immunoreactivity in wounds of WT and HO-2 KO mice at day 7 after wounding; bar, 200 μ m. (**D**) Semi-quantitative scoring of α SMA in (**C**) presented as box-and-whisker plot with 10–90 percentiles.

wound area. Differential expression of HO-1 and HO-2 in keratinocytes and fibroblasts has been demonstrated [42]. This difference is critical for different sensitivities towards UV-induced oxidative stress [15, 43]. This could also have consequences in a more complex setting, such as during wound repair. However, we did not observe any differences between HO-2 KO and WT mice with respect to the proliferation marker Ki67 or expression of the myofibroblast marker α SMA during the time course of wound healing.

Angiogenesis is a crucial process for proper wound healing, and disturbed blood vessel formation leads to delayed wound healing. Pro-angiogenic properties of HO-1 have been demonstrated [20, 21]. Both diabetic db/db mice having weaker injury-induced HO-1 expression and HO-1 deficient mice demonstrate impaired vascularization and delayed wound closure which could be restored with HO-1 gene transfer [12]. Here, we also observed lower vessel density in the wounds of HO-2 KO mice despite normal HO-1 expression. This may restrict the blood supply to the healing tissue and set back wound healing.

To probe the molecular mechanism responsible for the delayed cutaneous wound closure in HO-2 KO mice, we used a PCR array containing 84 wound healing associated genes. Surprisingly, we only detected significant differences between HO-2 KO and WT mice in the expression profile of a single gene, namely CXCL-11. CXCL-11 is a

versatile cytokine that *via* interaction with its receptor CXCR3 is thought to modulate several cell types important during several phases of cutaneous wound repair [44]. Decreased CXCL-11 or CXCR3 expression leads to delayed re-epithelization, impaired epidermis maturation and is associated with altered angiogenesis [45–48]. CXCL-11 is also an antagonist for C-C chemokine receptor type 5 (CCR5) [49]. CCR5 KO mice have delayed wound closure, impaired neovascularization and reduced collagen production following excisional wounding [50]. In contrast to WT controls, we did not detect any injury-induced up-regulation of CXCL-11 mRNA in HO-2 KO mice at day 2 after wounding. But, surprisingly, more CXCL-11 positive cells were present in the wounds of HO-2 KO mice compared to WT controls at day 7 after wounding. These observations imply that there is a slight delay in the expression of CXCL-11 gene and protein in HO-2 KO mice compared to WT controls. However, whether this is a consequence or a causing factor of the delayed cutaneous wound closure in HO-2 KO mice warrants further investigation. Summarizing, we demonstrated delayed dermal wound closure, decreased vascularization and reduced collagen deposition in HO-2 KO mice independent from inflammation and HO-1 expression. These data indicate a tissue-specific role for HO-2, as HO-2 seems to play a pivotal role in corneal, but not cutaneous, wound healing. This is directly linked to the

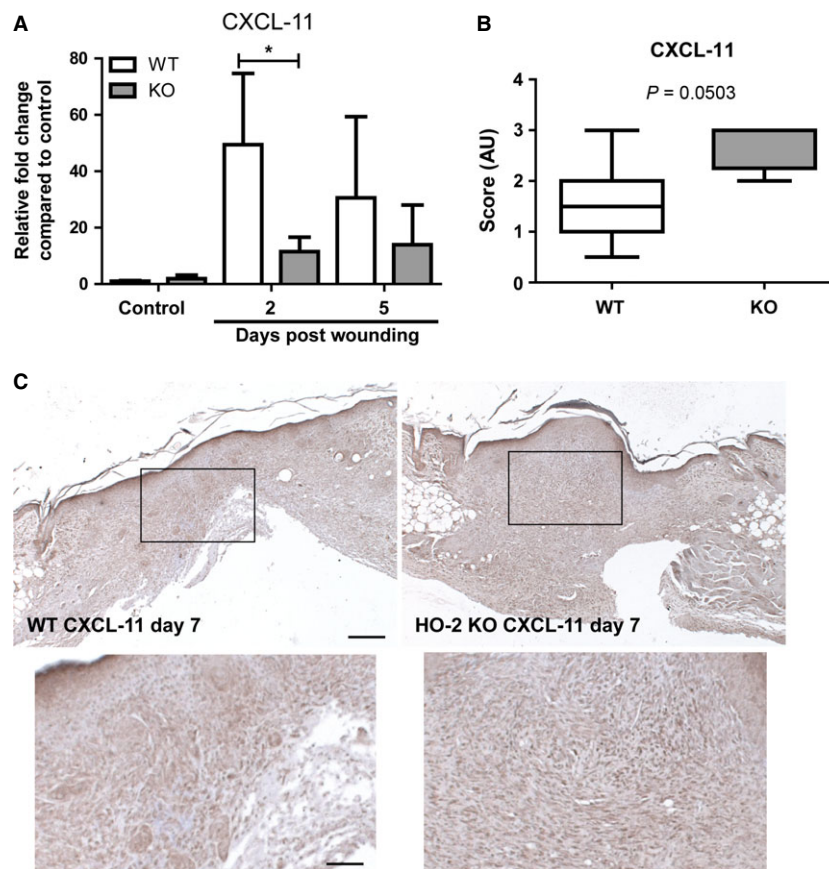


Fig. 6 Different CXCL-11 expression in HO-2 KO and WT mice after injury. **(A)** CXCL-11 gene transcript levels in WT (white bars) and HO-2 KO (grey bars) mice in time presented as mean \pm SD. Controls represent biopsies collected at day 0, and data were normalized to WT mean day 0. **(B)** Semi-quantitative scoring of CXCL-11 immunoreactivity in **(C)** of WT (white) and HO-2 KO (grey) wounds presented as box-and-whisker plot with 10–90 percentiles. $*P < 0.05$. **(C)** Representative images of CXCL-11 immunoreactivity in wound tissue of WT and HO-2 KO mice at day 7 after wounding; bar, 200 μ m. Insert represent magnified boxed area; bar, 70 μ m.

regulation of injury-induced HO-1 expression. Furthermore, we report differences in the expression of the cytokine CXCL-11 between HO-2 KO and WT mice during wound repair. Whether this difference is causative or caused by the observed delay in cutaneous wound closure needs to be further investigated.

Acknowledgements

The authors thank Dr. J. Von den Hoff for helpful discussion on the statistics. This study was supported by the Dutch Burns Foundation (# 09.110) and TASENE (NWO/SIDA/COSTECH W02.29.101).

Conflicts of interest

The authors confirm that there are no conflicts of interest.

Author contribution

DMSL, AS, NAJC, SWCP, JP, RR and CRB performed the research. RFR provided the KO mice for the study. DMSL, AS and FADTGW designed the study. DMSL, AS, RR and JM analysed the data. DMSL, CEC, FGMR and FADTGW wrote the manuscript. All authors approved the final version of the manuscript.

Supporting information

Additional Supporting Information may be found in the online version of this article:

Figure S1 Cutaneous HO-2 expression in WT and HO-2 KO mice.

References

- Martin P. Wound healing—aiming for perfect skin regeneration. *Science*. 1997; 276: 75–81.
- Buganza Tepole A, Kuhl E. Systems-based approaches toward wound healing. *Pediatr Res*. 2013; 73: 553–63.
- Sidgwick GP, Bayat A. Extracellular matrix molecules implicated in hypertrophic and keloid scarring. *J Eur Acad Dermatol Venerol*. 2012; 26: 141–52.
- Grice EA, Segre JA. Interaction of the microbiome with the innate immune response in chronic wounds. *Adv Exp Med Biol*. 2012; 946: 55–68.
- Otterbein LE, Choi AM. Heme oxygenase: colors of defense against cellular stress. *Am J Physiol Lung Cell Mol Physiol*. 2000; 279: L1029–37.
- Maines MD, Trakshel GM, Kutty RK. Characterization of two constitutive forms of rat liver microsomal heme oxygenase. Only one molecular species of the enzyme is inducible. *J Biol Chem*. 1986; 261: 411–9.
- Grochot-Przeczek A, Dulak J, Jozkowicz A. Haem oxygenase-1: non-canonical roles in physiology and pathology. *Clin Sci*. 2012; 122: 93–103.
- Willis D, Moore AR, Frederick R, et al. Heme oxygenase: a novel target for the modulation of the inflammatory response. *Nat Med*. 1996; 2: 87–90.
- Abraham NG, Kappas A. Pharmacological and clinical aspects of heme oxygenase. *Pharmacol Rev*. 2008; 60: 79–127.
- Yachie A, Niida Y, Wada T, et al. Oxidative stress causes enhanced endothelial cell injury in human heme oxygenase-1 deficiency. *J Clin Invest*. 1999; 103: 129–35.
- Kapturczak MH, Wasserfall C, Brusko T, et al. Heme oxygenase-1 modulates early inflammatory responses: evidence from the heme oxygenase-1-deficient mouse. *Am J Pathol*. 2004; 165: 1045–53.
- Grochot-Przeczek A, dLach R, Mis J, et al. Heme oxygenase-1 accelerates cutaneous wound healing in mice. *PLoS ONE*. 2009; 4: e5803.
- Seta F, Bellner L, Rezzani R, et al. Heme oxygenase-2 is a critical determinant for execution of an acute inflammatory and reparative response. *Am J Pathol*. 2006; 169: 1612–23.
- Bellner L, Wolstein J, Patil KA, et al. Biliverdin rescues the HO-2 null mouse phenotype of unresolved chronic inflammation following corneal epithelial injury. *Invest Ophthalmol Vis Sci*. 2011; 52: 3246–53.
- Zhong JL, Raval C, Edwards GP, et al. A role for Bach1 and HO-2 in suppression of basal and UVA-induced HO-1 expression in human keratinocytes. *Free Radic Biol Med*. 2010; 48: 196–206.
- Dennerly PA, Spitz DR, Yang G, et al. Oxygen toxicity and iron accumulation in the lungs of mice lacking heme oxygenase-2. *J Clin Invest*. 1998; 101: 1001–11.
- Ding Y, Zhang YZ, Furuyama K, et al. Down-regulation of heme oxygenase-2 is associated with the increased expression of heme oxygenase-1 in human cell lines. *FEBS J*. 2006; 273: 5333–46.
- Ahanger AA, Prawez S, Leo MD, et al. Pro-healing potential of hemin: an inducer of heme oxygenase-1. *Eur J Pharmacol*. 2010; 645: 165–70.
- Bellner L, Vitto M, Patil KA, et al. Exacerbated corneal inflammation and neovascularization in the HO-2 null mice is ameliorated by biliverdin. *Exp Eye Res*. 2008; 87: 268–78.
- Bussolati B, Ahmed A, Pemberton H, et al. Bifunctional role for VEGF-induced heme oxygenase-1 *in vivo*: induction of angiogenesis and inhibition of leukocytic infiltration. *Blood*. 2004; 103: 761–6.
- Bussolati B, Mason JC. Dual role of VEGF-induced heme-oxygenase-1 in angiogenesis. *Antioxid Redox Signal*. 2006; 8: 1153–63.
- Poss KD, Thomas MJ, Ebralidze AK, et al. Hippocampal long-term potentiation is normal in heme oxygenase-2 mutant mice. *Neuron*. 1995; 15: 867–73.
- Tan SD, Xie R, Klein-Nulend J, et al. Orthodontic force stimulates eNOS and iNOS in rat osteocytes. *J Dent Res*. 2009; 88: 255–60.
- Gal P, Toporcer T, Vidinsky B, et al. Early changes in the tensile strength and morphology of primary sutured skin wounds in rats. *Folia Biol*. 2006; 52: 109–15.
- Faragalla HF, Marcon NE, Yousef GM, et al. Immunohistochemical staining for smoothelin in the duplicated versus the true muscularis mucosae of Barrett esophagus. *Am J Surg Pathol*. 2011; 35: 55–9.
- Park SS, Yang JI, Kim SK, et al. Positive effects of orally administered sildenafil on skin wound healing of rats. *TERM*. 2010; 7: 425–31.
- Hadi AM, Mouchaers KT, Schaliij I, et al. Rapid quantification of myocardial fibrosis: a new macro-based automated analysis. *Cell Oncol*. 2011; 34: 343–54.
- Livak KJ, Schmittgen TD. Analysis of relative gene expression data using real-time quantitative PCR and the 2(-Delta Delta C (T)) Method. *Methods*. 2001; 25: 402–8.
- Scharstuhl A, Mutsaers HA, Pennings SW, et al. Curcumin-induced fibroblast apoptosis and *in vitro* wound contraction are regulated by antioxidants and heme oxygenase: implications for scar formation. *J Cell Mol Med*. 2009; 13: 712–25.
- Barsky SH, Baker A, Siegal GP, et al. Use of anti-basement membrane antibodies to distinguish blood vessel capillaries from lymphatic capillaries. *Am J Surg Pathol*. 1983; 7: 667–77.
- Gerdes J, Lemke H, Baisch H, et al. Cell cycle analysis of a cell proliferation-associated human nuclear antigen defined by the monoclonal antibody Ki-67. *J Immunol*. 1984; 133: 1710–5.
- Eming SA, Krieg T, Davidson JM. Inflammation in wound repair: molecular and cellular mechanisms. *J Invest Dermatol*. 2007; 127: 514–25.
- Wagener FA, Volk HD, Willis D, et al. Different faces of the heme-heme oxygenase system in inflammation. *Pharmacol Rev*. 2003; 55: 551–71.
- Kampfer H, Kolb N, Manderscheid M, et al. Macrophage-derived heme-oxygenase-1: expression, regulation, and possible functions in skin repair. *Mol Med*. 2001; 7: 488–98.
- Hanselmann C, Mauch C, Werner S. Haem oxygenase-1: a novel player in cutaneous wound repair and psoriasis? *Biochem J*. 2001; 353: 459–66.
- Wagener FA, da Silva JL, Farley T, et al. Differential effects of heme oxygenase isoforms on heme mediation of endothelial intracellular adhesion molecule 1 expression. *J Pharmacol Exp Ther*. 1999; 291: 416–23.
- Wagener FA, van Beurden HE, von den Hoff JW, et al. The heme-heme oxygenase system: a molecular switch in wound healing. *Blood*. 2003; 102: 521–8.
- Patil K, Bellner L, Cullaro G, et al. Heme oxygenase-1 induction attenuates corneal inflammation and accelerates wound healing after epithelial injury. *Invest Ophthalmol Vis Sci*. 2008; 49: 3379–86.
- Marrazzo G, Bellner L, Halilovic A, et al. The role of neutrophils in corneal wound healing in HO-2 null mice. *PLoS ONE*. 2011; 6: e21180.
- Adachi T, Ishikawa K, Hida W, et al. Hypoxemia and blunted hypoxic ventilatory responses in mice lacking heme oxygenase-2.

- Biochem Biophys Res Commun.* 2004; 320: 514–22.
41. **Bellner L, Martinelli L, Halilovic A, et al.** Heme oxygenase-2 deletion causes endothelial cell activation marked by oxidative stress, inflammation, and angiogenesis. *J Pharmacol Exp Ther.* 2009; 331: 925–32.
 42. **Applegate LA, Noel A, Vile G, et al.** Two genes contribute to different extents to the heme oxygenase enzyme activity measured in cultured human skin fibroblasts and keratinocytes: implications for protection against oxidant stress. *Photochem Photobiol.* 1995; 61: 285–91.
 43. **Zhong JL, Edwards GP, Raval C, et al.** The role of Nrf2 in ultraviolet A mediated heme oxygenase 1 induction in human skin fibroblasts. *Photochem Photobiol Sci.* 2010; 9: 18–24.
 44. **Davidson JM.** Can scarring be turned off? *Am J Pathol.* 2010; 176: 1588–91.
 45. **Dale DC, Boxer L, Liles WC.** The phagocytes: neutrophils and monocytes. *Blood.* 2008; 112: 935–45.
 46. **Yates CC, Whaley D, Y-Chen A, et al.** ELR-negative CXC chemokine CXCL11 (IP-9/ITAC) facilitates dermal and epidermal maturation during wound repair. *Am J Pathol.* 2008; 173: 643–52.
 47. **Yates CC, Whaley D, Hooda S, et al.** Delayed reepithelialization and basement membrane regeneration after wounding in mice lacking CXCR3. *Wound Repair Regen.* 2009; 17: 34–41.
 48. **Yates CC, Whaley D, Kulasekaran P, et al.** Delayed and deficient dermal maturation in mice lacking the CXCR3 ELR-negative CXC chemokine receptor. *Am J Pathol.* 2007; 171: 484–95.
 49. **Petkovic V, Moghini C, Paoletti S, et al.** ITAC/CXCL11 is a natural antagonist for CCR5. *J Leukoc Biol.* 2004; 76: 701–8.
 50. **Ishida Y, Kimura A, Kuninaka Y, et al.** Pivotal role of the CCL5/CCR5 interaction for recruitment of endothelial progenitor cells in mouse wound healing. *J Clin Invest.* 2012; 122: 711–21.
 51. **Wang H, Yan S, Chai H, et al.** Shear stress induces endothelial transdifferentiation from mouse smooth muscle cells. *Biochem Biophys Res Commun.* 2006; 346: 860–5.